Society of Petroleum Engineers

SPE-229027-MS

Reservoir Mapping While Drilling Using Ultra-Deep Azimuthal Resistivity

A. Hartmann, U. Peikert, M. Linke, G. Dyatlov, and Yu. Antonov, Baker Hughes, Celle, Germany; H. Andersson, Baker Hughes, Copenhagen, Denmark; W. Fernandes, Baker Hughes, Celle, Germany

 DOI 10.2118/229027-MS

This paper was prepared for presentation at the ADIPEC held in Abu Dhabi, UAE, 3 – 6 November 2025.

Abstract

Geosteering horizontal wells has been a long-standing practice, in particular where seismic uncertainty is large. Conventional logging-while-drilling resistivity tools detect remote layers several meters away from the wellbore, sufficient to place the wellbore accurately relative to a formation boundary. However, operators today want to understand the full reservoir architecture and need deep mapping technology to do so.

An electromagnetic logging-while-drilling system has been designed to meet this requirement and map multiple boundaries up to 300 ft away from the wellbore. This is achieved by a modular design with flexible placement of transmitters and receivers in the bottom hole assembly (BHA) and a wide range of low and high frequencies. The system measures the full magnetic coupling tensor using the induction logging principle.

Data analysis is based on 1D or multidimensional inversion of the acquired data. 1D algorithms are based on a semi-analytical solver coupled with a statistics-enhanced Levenberg-Marquardt algorithm for inversion. More advanced algorithms use a pixel-based FEM solver coupled with the same inversion engine and may be needed in complex geologies. An inversion workflow combines both systems for real-time mapping of reservoir boundaries.

The system performance was modeled in order to define the needed system specifications. Frequencies, spacings, and coil dipole moments were defined based on the modeling. The system was then built and verified in the lab. It was deployed in a test well in Germany to verify the modeled performance. Data was compared to a well-established logging tool, confirming the enhanced mapping capabilities of the new system in this environment.

Detection of remote boundaries could be enhanced significantly with this new service by not only increasing the depth of detection, but also by improving the resolution of thin layers above the main target.

Introduction

In the early 2000's, the usage of ultra-deep resistivity started on the Norwegian Grane field (Helgesen et al. 2005; Iversen et al. 2003). It was successfully used in thick, homogeneous reservoirs to place wells above the oil-water contact and underlying shales. Interpretational models were reasonably simple in these environments (Gravem et al. 2006; Helgesen et al. 2005a).The application was then extended to reservoir navigation in channelized sands (Tilsley-Baker at al 2013). The complex geology required more advanced

interpretation capabilities (Sviridov et al. 2012), introducing a layered geology inversion of electromagnetic data. Subsequently the interpretation in this environment was further improved by introducing azimuthal measurements (Tilsley-Baker at al. 2015). This resulted in ultra-deep azimuthal resistivity tools (UDAR) (Seydoux et al. 2014; Hartmann et al. 2014; Bittar et al. 2018).

Nowadays, UDAR has proven its value in numerous deployments. Fig. 1 shows main application scenarios. The large depth of detection allows detecting remote reservoirs and landing or geostopping wells safely without pilot wells. Multi boundary mapping provides the confidence to place the well optimally in complex geologies like channelized sands. In general the mapping capabilities are used to define the reservoir geometry, map remote boundaries, and inform the operator about the reservoir architecture (Gezeery et al. 2017; Holmquist et al. 2025.; Al-Ansari et al. 2024).

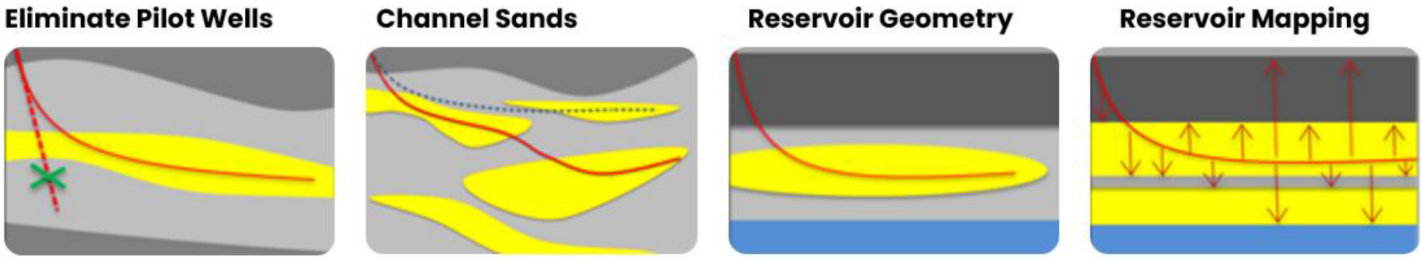

Figure 1—Typical application scenarios for UDAR services.

The need for even more comprehensive data sets in increasingly complex geologies requires constant improvements. Building on previous developments has led to the design of a new UDAR system capable of advanced reservoir mapping. The following section describes the design of the downhole system, followed by the description of the interpretation software. Finally, an application of the new system in a test well in Germany concludes the discussion.

Measurement System

A new downhole system was designed with the target to take proven design concepts of the existing UDAR hardware but enhance it to provide a much richer data set for interpretation. This required a complete rethinking of the system (Fig. 2). The new UDAR tool is built as a modular transceiver, requiring only one type of tool on the rig site. The transceivers support flexible configurations that allow advanced acquisition modes. Each transceiver module features a tri-axial antenna array. The array consists of high moment, true cross-component tri-axial antennas. This design is the first in the industry featuring colocated, pure component tri-axial antennas. Because the tensor components do not have to be extracted by transformations from tilted mixed signals, true cross-components allow for better signal to noise ratios and achieve larger depth of detections with small transmitter-receiver spacings (Zhou 2009). Due to the induction nature, induced voltages at receivers are proportional to the transmitted frequency. High moment antennas are important for accurately measuring lower frequency signals down to the kHz range with sufficient signal-to-noise ratio. This allows larger transmitter-receiver spacings for greater depth of detection even in unfavorable low resistivity environments.

Figure 2—Downhole measurement module of the new UDAR system. Co-located true Z/X/Y antennas are shown in the antenna section.

The UDAR system/service consists of the low-frequency modular tools combined with a conventional azimuthal propagation resistivity (APR) tool whose measurements are used to characterize the near wellbore

environment. The range of available frequencies is shown in Table 1. The high-frequency range is covered by the APR tool. Mid- and low-frequency ranges are provided with 3 frequencies per decade by the UDAR modules. For special applications, an ultra-low frequency below 1 kHz is available.

Table 1—Frequency ranges of the new UDAR downhole system. Ultra-low to mid frequency range is delivered by the modular UDAR system. High frequency is delivered by the MPR system.

Frequency range (kHz)	Category
<= 1	Ultra Low Frequency
>1 - 10	Low Frequency
>10 - 100	Mid Frequency
> 100 – 2000	High Frequency

A typical BHA is shown in Fig. 3. Three modules are placed with increasing distance in the BHA. The short spacing M1-M2 covers the proximity close to the bit whereas a larger spacing is achieved using M1-M3. An APR tool can be placed in between the first two modules or below the first module, depending on the application requirements.

Figure 3—Placement of UDAR modules within a typical LWD BHA.

The capabilities of the new hardware have been extensively modeled and tested. One key metric of this type of measurement is the depth of detection (DoD). Several methods are used in the industry to define the value. Here, sensitivity of the measured signals to a remote boundary is used to define DoD. This is particularly clear for true cross-components. Fig. 4 illustrates the process of defining DoD. In the absence of a remote boundary, no cross-component signal will be measured, only the system-internal noise. When a boundary is approaching, the remote signal will eventually stand out from the system-internal noise. Reaching this point is defined as the depth of detection (Fig. 4). This process also illustrates the benefit of pure X/Y/Z measurements. Only one receiving antenna defines the noise floor, making it possible to record even very small signals from remote boundaries. Using mixed signals, cross-component signals are dominated by noise from co-axial signals. It is interesting to define DoD for a range of spacings, an example of this process is shown for low frequency range ZZ components in Fig. 5. The plot shows that depth of detection is not only increased by lowering the frequency, but also by increasing the transmitter-receiver spacing, in this case up to 90 m. The spacing dependency highlights the need for an acquisition system with high antenna moment and sensitivity. The example also shows the decrease of DoD for shorter spacings and higher frequencies. These signals play an important role in defining the resistivity structure closer to the wellbore.

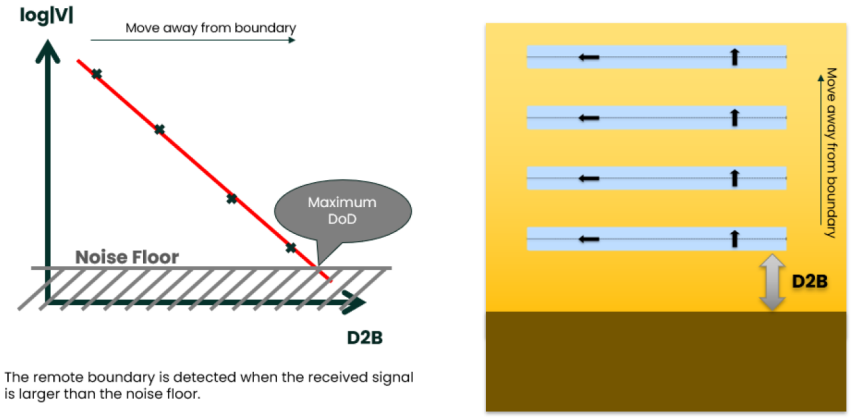

Figure 4—Principle of defining Depth of Detection for true cross-components in a two-layer configuration. The transmitter-receiver system is placed at increasing distances from the boundary, resulting in successively decreasing received voltages. Maximum DoD is the point where noise has the same magnitude as the boundary signal.

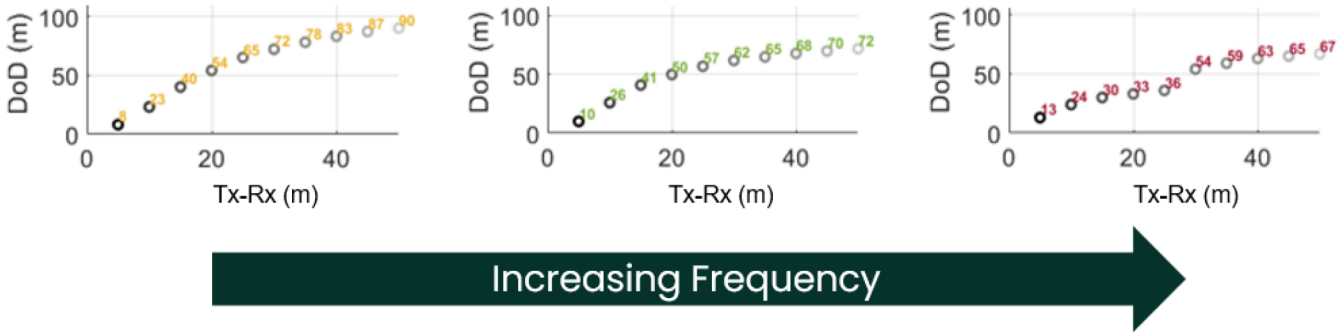

Figure 5—Depth of Detection for co-axial components for a resistivity contrast 100 ohm.m:1 ohm.m. DoD's are computed for three low-range frequencies. Lowering the frequency as well as increasing the spacing increases DoD.

Data Inversion and Interpretation

The inversion algorithms have been developed along with the UDAR tools, driven by the increasing number of measurements and HPC capabilities. However, the following features are common for all inversions. The resistivity distribution in the reservoir is sought in a certain model class (1D, 2D, or 3D). The model parameters are optimized using the Levenberg-Marquardt (or other gradient) method to attain the match between the measured and synthetic tool responses and meet the natural regularization conditions. Since the length of the wellbore is much greater than the depth of investigation (DOI) the inversion is performed interval by interval and the results from all intervals are combined into a reservoir model. Although composed of the local 1D layer-cake models, the whole model is 3D, because the measurements are naturally 3D and individual 1D models have arbitrary spatial orientations that are reconstructed by inversion. Very often inversion based on 1D local model efficiently maps substantial lateral changes of the subsurface structure.

With the introduction of UDAR technology, the feasibility and pre-well phases got additional importance and focus. To address inevitable limitations related to the mud-pulse telemetry bandwidth, an in-depth analysis is performed to identify the optimal set of measurements depending on the expected environmental challenges and according to the objectives of a particular job. Forward modeling, sensitivity and confidence analysis, depth-of-detection calculation, inversion, and statistical analysis of intermediate inversion models are carried out for numerous anticipated scenarios. Finally, the best set of measurements is selected based on detection and resolution confidence. Thanks to the availability of true components, the selection is made not only among the frequency range, but also across particular components.

Most cases are covered by the 1D inversion utilizing the layer-cake model. This model is parametrized by the layer thickness, resistivity, anisotropy, relative dip, and azimuth. Even in the cases of complex reservoirs, where the multi-dimensional inversion is required, we start with the 1D inversion. The choice of the number of layers, constraints, the data interval overlaps, and other parameters of inversion may vary to fit the objectives of the job. The well-known advantage of the semi-analytic 1D solver is its high performance which makes it possible to use thousands of initial guesses to thoroughly scan the model parameter domain. Comprehensive inversion quality control is done for every interval during real-time operations. It includes an essential check of the data match and extensive statistical analysis of the intermediate inversion models. The statistical resistivity distribution, obtained from multiple initial guesses and inversion steps on every inversion interval, yields the resistivity profile quantiles and demonstrates uncertainty of resistivity and boundary positions. Our experience shows that "best-match" model and statistically derived models complement each other. The best-match model usually gives good first indications of the approaching anomalies, while the statistical distribution looks less erratic. This improves the ability to map boundaries. To have a holistic view on the subsurface environment and make informed decisions, we recommend joint use of these deliverables. The results are displayed in a traditional 2D curtain section view and in a full 3D view for in-depth spatial analysis.

In complex reservoirs with abrupt and fast lateral changes like faults and unconformities, the 1D inversion leads to artifacts that are difficult to interpret correctly. The main non-1D indicators are: 1) Discontinuity of the inversion results on the neighboring intervals, 2) poor data match and specific behavior of the azimuthal measurement, and 3) when directional components of signals for different frequencies and spacings diverge. Like in the 1D inversion, the multi-dimensional workflow processes data interval by interval. However, since the multi-dimensional models have greater generality, they can explain larger intervals (up to 100 m) of measured data by a single model. The multi-dimensional models have much greater variety as compared with the 1D models: 2D or 3D, parametric or cell based, the grid orientation maybe fixed or not, etc. The choice of the model to be used in inversion is driven by the trade-off between the generality and resolution of the model and the speed of the corresponding multi-dimensional solver. The latter is the key consideration for real-time inversion. We use the 2D/3D anisotropic pixel-based model, i.e., the model with the variable orientation of the grid that can be changed manually or optimized during inversion automatically. On the one hand, it covers most non-1D situations, including longitudinal and oblique faults, with resolution up to 1 m. On the other hand, the performance achieved by parallelization and utilization of multi-GPU's and cloud computations makes it applicable in real-time even with numerous and wide range UDAR measurements. The initial model for multi-dimensional inversion is built based on the 1D inversion results, as it already captures the major features of the reservoir model. Then the resistivity of the cells and the grid orientation are optimized to fit the measured data. The resulting optimized orientation itself brings important information about the reservoir. The resulting 2D/3D models from different intervals are combined into the comprehensive 3D volume reservoir model. The whole inversion workflow is schematically shown in Fig. 6. Various presentations of the 3D volume are also provided: curtain section, transverse views, volumes with a certain resistivity threshold, etc.

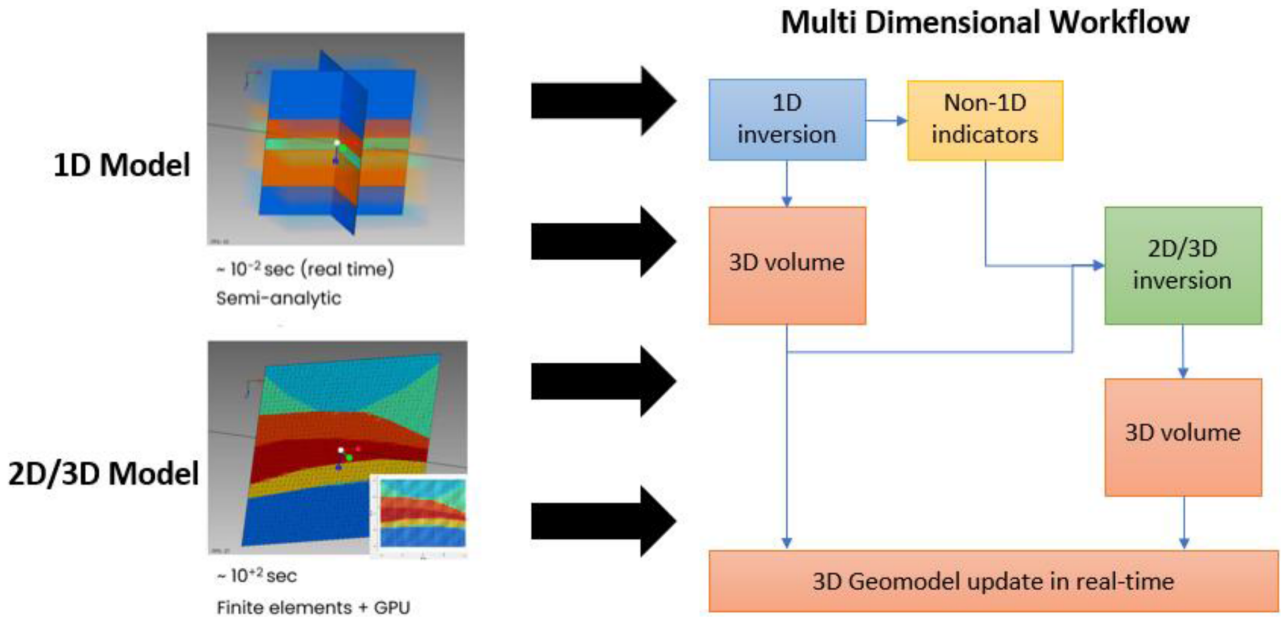

Figure 6—Multi dimensional inversion workflow. Left: Variable complexity models make up individual model building blocks. Right: Combination of individual models into an integrated multi-dimensional workflow.

Field Example

The new UDAR system was deployed on a dedicated test rig (Fig. 7, right). The rig is located about 15 km east of Celle, Germany. The purpose was to test the functionality of the entire service in real-time as well as confirm the prognosed depth-of-detection capabilities. Two test horizons are available in the Late Cretaceous and Late Triassic (Fig. 8, left). For testing DoD in a landing section, a salt layer in the lower test horizon was selected as target (Fig. 8, right). The top salt presents a resistivity contrast emulating a reservoir entry. The entry is complicated by the thin high resistive layers above the main target. A 50° tangent was drilled through the overburden and salt to map the target while landing and map top salt from below. The BHA used consisted of two UDAR modules plus a conventional MPR tool in addition to the RSS and Power/Telemetry tool (Fig. 7, left).

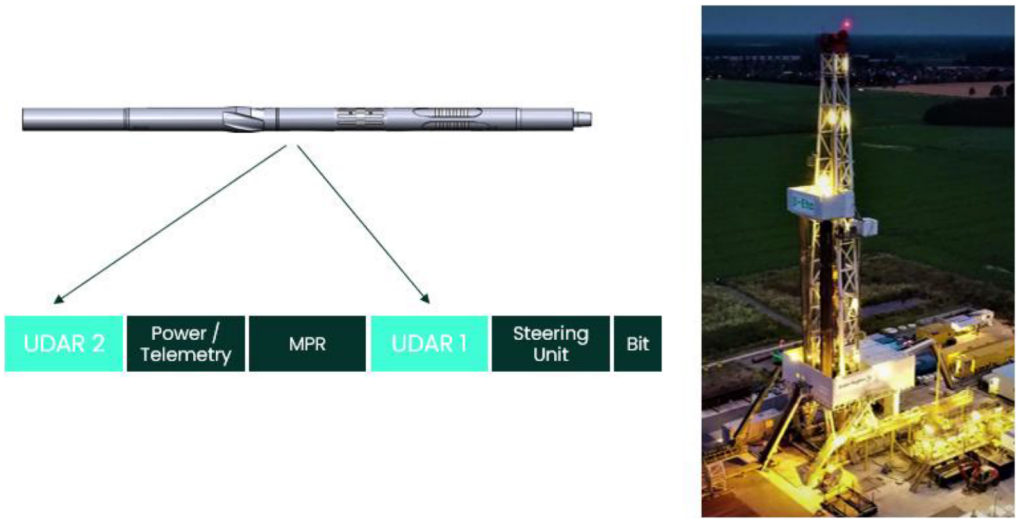

Figure 7—BHA deployment on the UDAR field test. Left: Setup of test BHA utilizing two UDAR modules. Right: Test rig in Germany that was used to deploy the UDAR BHA.

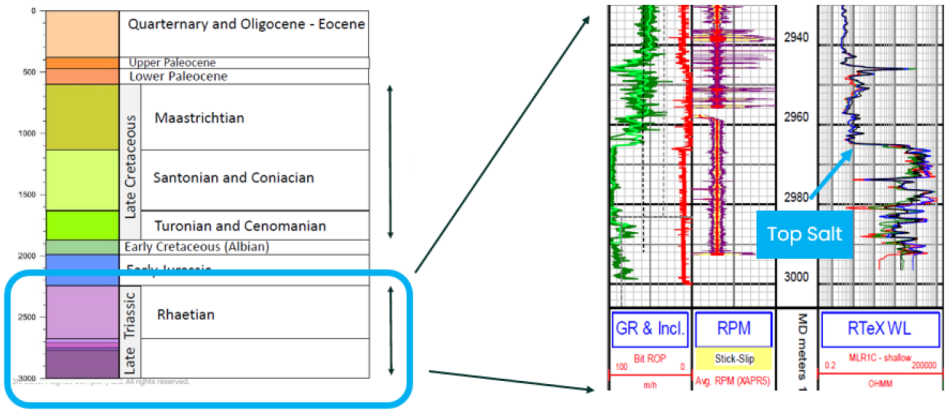

Figure 8—Test well overview. Left: Geologic cross section of the well showing lower test horizon in the Late Triassic. Right: Resistivity log of the target zone showing top salt and small resistive stringers above the main salt.

The geological layering is flat at this site. Therefore, a one-dimensional modeling code was used to create the pre-well model for the UDAR BHA. Fig. 9 shows the synthetic, normalized pre-well modeled data for the cross-component data of UDAR, together with MPR and APR data of the Deep Azimuthal Resistivity (DAR) tool. Visually, the rich response from the different components and frequencies can be appreciated. For a quick look, the deviation of the different signals from the homogeneous response shows the large increase in DoD by using an UDAR system over MPR and APR tools. The rich details show on the one hand the need for an advanced inversion, on the other hand the possibility to map detailed structures.

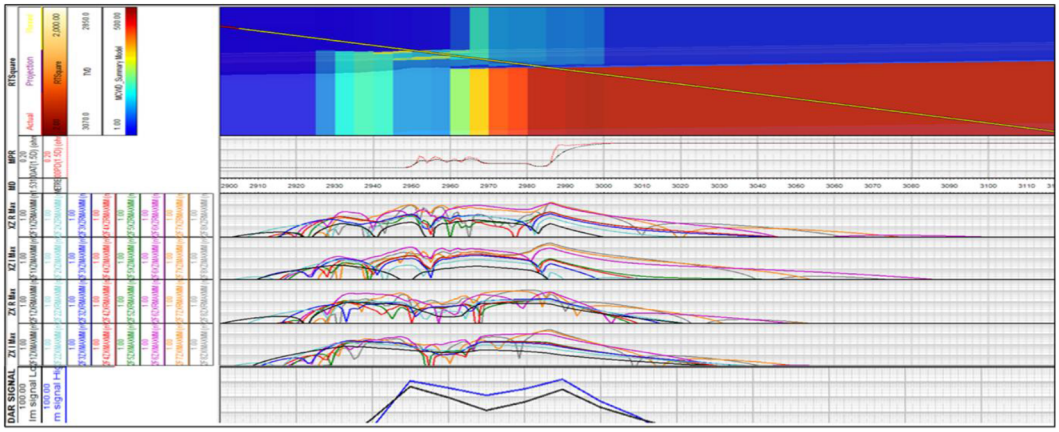

Figure 9—BETA pre-well model. Track 1: Resistivity cross section used for forward modeling. Track 2: Conventional resistivity MPR signals. Tracks 3 to 6: Selection of azimuthal signals from UDAR system. Track 7: Conventional APR signals. Comparing UDAR to APR and MPR signals, the increase in depth of detection can be visually appreciated as the point where signals deviate from the homogeneous response.

The BHA was deployed as planned and data was recorded and interpreted in real-time and memory. The focus here will be on the memory data. To analyze the memory data, two different workflows were utilized.

In the forward data analysis, a resistivity post-well model was built based on the conventional resistivity measurements. The data was then used to predict the UDAR response, without using UDAR itself in the prediction. The analysis was done successively for all curves to verify the predicted accuracy of the measurement system and identify any potential offsets or data issues. The comparison between measurement and prediction showed a very good match and consistency, shown exemplary for three co-axial components in Fig. 10. The section shows the normalized change in signal level when entering the salt layer. Small deviations are due to local variations in resistivity of the layered geology.

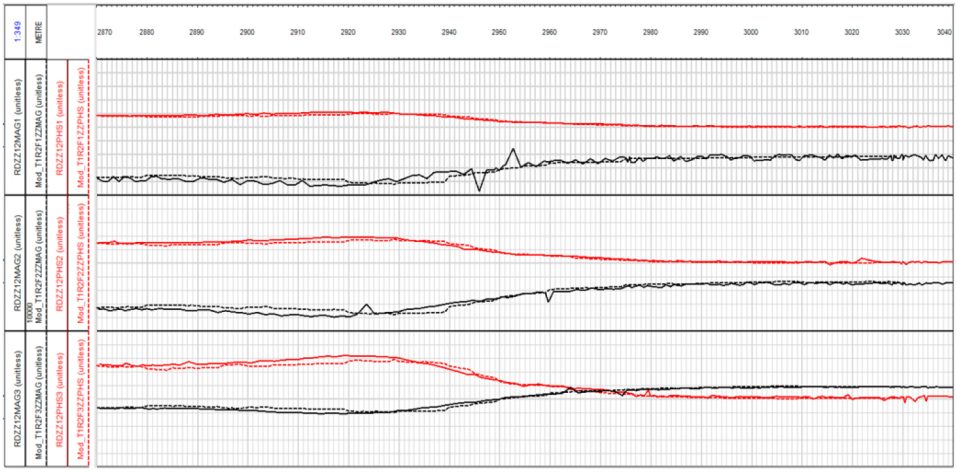

Figure 10—Forward data analysis example. Comparison of modelled data (dashed lines) based on conventional MPR data to measured UDAR data (solid lines). Data is shown for lower three frequencies.

In the inverse analysis, an inverse model was created using first a subset of co-axial data. Then additional curves were subsequently added and the inverse analysis repeated. The resulting data match, correctness of the resulting model, and consistency of the results were assessed. Adding of curves and analyzing the results were repeated until all curves were used. This process ensures all data and the inversion workflow meet the expected quality criteria. At the end, a final interpretation was created (Fig. 11). The thin resistive layer could be detected 25 m TVD ahead. The main resistivity contrast was also detected from 25 m TVD above the top of the salt layer, before drilling through the thin resistive layer. After entering the salt, thickness of the salt layer was consistently mapped at about 60 m thickness.

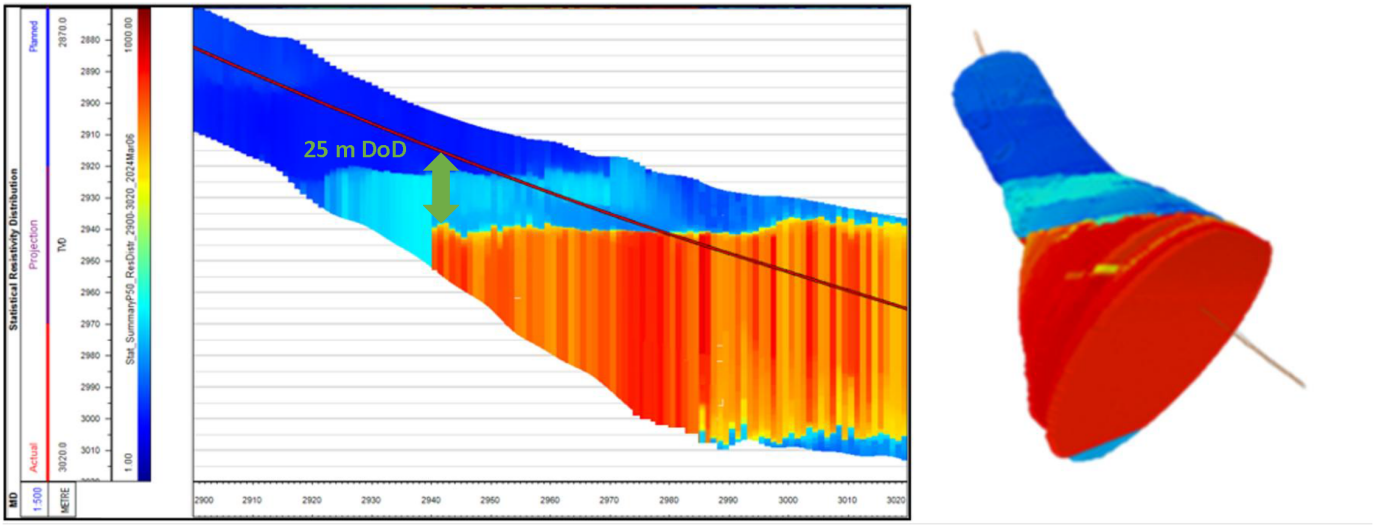

Figure 11—Inversion results for the landing section. Inversion results are cut off at the computed DoD tube. Left: 2D curtain section along the well trajectory. Top salt is resolved with 25 m depth of detection. As well as being able to differentiate the high resistivity target from the resistive stringer above the salt layer. Right: Integration of inversion results into the 3D volume. 3D view of the well trajectory and the resistivity volume, view direction is uphole from the toe of the well.

Conclusion

A new Ultra-Deep Azimuthal Resistivity system was developed to meet the increasing demand for EM based reservoir mapping. The LWD system uses for the first time colocated triaxial, pure-component antennas with high sensitivity. It measures the full magnetic coupling tensor enabling advanced inversion interpretation. The required depth of detection is established by allowing large transmitter-receiver spacings

and frequencies in the range of 1 kHz to 100 kHz. Data is then transmitted either in real-time to surface or recorded in memory. A new, multi-dimensional hybrid inversion workflow has been developed to support the interpretation of the data from the downhole UDAR tools. It allows a flexible choice of inversion strategy to efficiently create a multi-dimensional inversion result suitable for simple and complex geologies. Combining both key-developments with advanced 3D visualization, it is possible to derive the 3D resistivity map around the wellbore. The workflow can be deployed based on memory or real-time data, allowing the optimal wellbore placement as well as in-depth geological interpretation post-run.

The first ever deployment of the new system was executed on a dedicated test rig in Germany. The downhole system showed excellent performance, resulting in acquisition of a high-quality data set. This was verified by forward modeling and inversion analysis. Despite the heterogeneous geological environment and a relatively low inclination of 50°, the multi-dimensional inversion of the data set provided a very favorable depth of detection. The modules can be placed directly behind the steering unit, providing sufficient early warning to safely land or geostop the well. After internal testing the system was successfully deployed by several customers in Europe and the Middle East. The modules have now accumulated over 5000 circulation hours. In future, also advanced acquisition modes will be deployed, fully utilizing the benefits of the transceiver setup.

References

Al-Ansari, Y., Mumtaz, A., Potshangbam, S. et al 2024. Integration of Innovative Real-Time Extra-Deep Mapping Technology Maximizes Reservoir Exposure and Increased Production Potential of a Complex Reservoir - A Successful Case History from the Largest Onshore Field, Libya. ADIPEC, Abu Dhabi, UAE, 4-7 November. SPE-222267-MS. https://doi.org/10.2118/222267-MS.

Bittar, M., Campbell, A., Beeley, H. et al 2018. Optimal 3D Reservoir Insight with a new Ultra-Deep Reading Azimuthal LWD Resistivity Tool. SPE ATCE, Dallas, Texas, September 24-26. SPE-191433-MS. https://doi.org/10.2118/191433-MS.

Taher, E.-G., Wessling, S., Monirah, E.-J. et al 2019. Resolving True Formation Resistivity and Reconstructing Structural Reservoir Complexity using Resistivity Inversion in High Angle & Horizontal Wells to Gain Insights into Future Reservoir Production Behaviour and Devise Proactive Completion Strategy - A Case Study from Lower Burgan Formation, Minagish Field, West Kuwait. SPE Kuwait Oil & Gas Show and Conference, Mishref, Kuwait, 13-16 October. SPE-198044-MS. https://doi.org/10.2118/198044-MS.

Gravem, T., Thorsen, A. K., Helgesen, T. B. et al 2006. Multiple Advanced Logging-While-Drilling Technologies Optimized for Drilling and Well Placement. OTC. Houston, Texas, 1-4 May. OTC-18037-MS. https://doi.org/10.4043/18037-MS.

Hartmann, A., Vianna, A., Maurer, H.-M. et al 2014. Verification Testing of a new Extra-Deep Azimuthal Resistivity Measurement. SPWLA 55th Annual Logging Symposium. May 18-22, Abu Dhabi, UAE. SPWLA-2014-MM.

Helgesen, T. B., Fulda, C., Meyer, W. H. et al 2005. Reservoir Navigation with an Extra Deep Resistivity LWD Service. SPWLA 46th Annual Logging Symposium, New Orleans, Louisiana, June 26-29. SPWLA-2005-I.

Helgesen, T. B., Meyer, W. H., Thorsen, A. K. et al 2005a. Accurate Wellbore Placement Using a Novel Extra Deep Resistivity Service. SPE Europec/EAGE Annual Conference, Madrid, Spain, 13–16 June. SPE-94378-MS. https://doi.org/10.2118/94378-MS.

Holmquist, A. N., Khemissa, H., Agnihotri, P. et al 2025. Novel Multi-Dimension Inversion of Ultra-Deep Azimuthal Resistivity Service Allows Strategic Decision in Real-Time Enhancing Reservoir Management. GOTECH, Dubai City, UAE, April 21-23. SPE-224537-MS. https://doi.org/10.2118/224537-MS.

Iversen, M., Fejerskov, M., Skjerdingstad, A.-L. et al 2003. Geosteering Using Ultradeep Resistivity On The Grane Field, Norwegian North Sea. SPWLA 44th Annual Logging Symposium, Galveston, Texas, June 22-25. SPWLA-2003-J.

Seydoux, J, Legendre, E., Mirto, E. et al 2014. Full 3D Deep Directional Resistivity Measurements Optimize Well Placement and Provide Reservoir-Scale Imaging While Drilling. SPWLA 55th Annual Logging Symposium, May 18-22, Abu Dhabi, UAE. SPWLA-2014-LLLL.

Tilsley-Baker, R., Sviridov, M., Mosin, A. et al 2013. Extra Deep Resistivity Experience in Brazil Geosteering Operations. SPE ATCE, New Orleans, Louisiana, USA, September 30-October 2. SPE-166309-MS. https://doi.org/10.2118/166309-MS.

Tilsley-Baker, R., Hartmann, A., Sviridov, M. et al 2015. The Importance of Extra-Deep Azimuthal Resistivity in Reservoir Development: An Update on Recent Field Experiences. OTC Brazil, Rio de Janeiro, Brazil, October 27–29. OTC-26315-MS. https://doi.org/10.4043/26315-MS.

Sviridov, M.; Mosin, A.; Antonov, Yu. et al 2012. New Software for Processing of LWD Extra-Deep and Azimuthal Resistivity Data. Russian Oil & Gas Exploration & Production Technical Conference, Moscow, Russia, October 16-18. SPE-160257-MS. https://doi.org/10.2118/160257-MS.

Sviridov, M., Antonov, Yu., Martakov, S. et al 2019. Quality Control of LWD Resistivity Data Inversion Results. SPE ATCE, Calgary, Alberta, Canada, September 30-October 2. SPE-195817-MS. https://doi.org/10.2118/195817-MS

Zhou, J. Q., 2009. On the Depth of Investigation – Achieving Deeper Investigation with Shorter Source - Receiver Spacing. *Petrophysics* **50**(5): 427–429. SPWLA-2009-v50n5a4.